International Journal of Materials and Chemistry 2025, 15(4): 77-82
DOI: 10.5923/j.ijmc.20251504.02

Physico–Chemical Analysis of Palladium and Al_2O_3 Support After Regeneration: SEM, EDS, and XRD Studies

Feruza Tursunova[1], Mukhtar Amonov[2], Uktam Mardonov[3]

[1]PhD Student, Bukhara State Technical University, Bukhara, Uzbekistan
[2]Professor, Bukhara State University, Bukhara, Uzbekistan
[3]Associate Professor, Bukhara State University, Bukhara, Uzbekistan

Abstract This study presents a detailed physicochemical investigation of regenerated palladium and γ-Al_2O_3 catalyst supports following leaching and reduction processes. Advanced analytical techniques – scanning electron microscopy (SEM), energy-dispersive X-ray spectroscopy (EDS), and X-ray diffraction (XRD)–were employed to assess morphology, phase composition, and impurity distribution. The SEM and EDS analyses revealed that residual sulfur, chlorine, and zinc impurities remained after acid leaching and zinc reduction, accounting for up to 22–25% of total contaminants, while the palladium concentration increased from 1.4–2.6% in the spent catalyst to 70–85% in the regenerated product. Comparative XRD data confirmed the preservation of the γ-Al_2O_3 crystalline phase and the reduction of oxidized palladium species to metallic Pd^0, indicating structural restoration of the catalyst and its support. The findings suggest that substituting zinc powder with sodium formate or hydrazine hydrate as reducing agents can yield higher purity (≈98%) palladium with minimal secondary contamination. Overall, the comprehensive SEM–EDS–XRD characterization demonstrates that optimized regeneration effectively restores the catalyst's morphological stability, metal dispersion, and phase integrity, enabling its repeated reuse in industrial applications with improved economic and environmental efficiency.

Keywords Palladium regeneration, γ-Al_2O_3 support, SEM, EDS, XRD, Catalyst recycling, Hydrometallurgy, Purity enhancement

1. Introduction

Effective recycling of spent catalysts is impossible without assessing the physic–chemical characteristics of the recovered metal and support. Modern quality requirements for secondary Pd necessitate the mandatory use of analytical techniques such as scanning electron microscopy (SEM), energy–dispersive X–ray spectroscopy (EDS), and X–ray diffraction (XRD). Global practice confirms that these methods allow not only monitoring the degree of purification but also optimizing the choice of reducing agents [1,2,3,4].

The palladium precipitate and residual γ–Al_2O_3 remaining after acid leaching and zinc reduction were used.

For effective regeneration and metal recovery, it is important to take into account the altered catalyst composition, especially the composition and structural features of the accumulated contamination and carrier degradation.

Received: Oct. 8, 2025; Accepted: Oct. 27, 2025; Published: Nov. 19, 2025
Published online at http://journal.sapub.org/ijmc

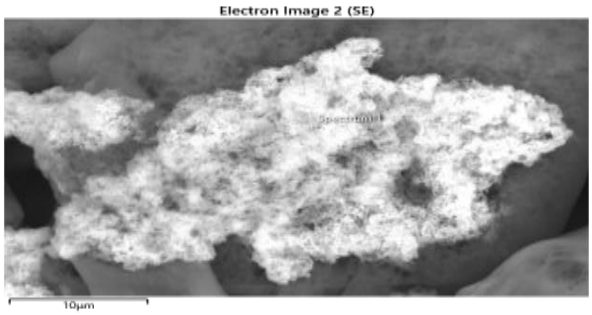

Figure 1. 1–point SEM analysis of the isolated Pd sample

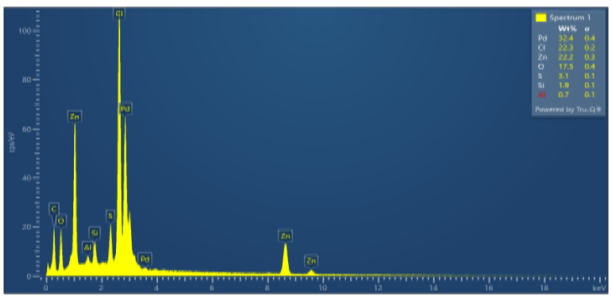

Figure 2. 1–point SEM spectrum of the isolated Pd sample

2. Materials and Methods

The experimental studies were conducted using spent Pd/γ-Al_2O_3 catalyst samples (G–58I) obtained from industrial hydrogenation processes. The initial catalyst contained about 1.4–2.6 wt% palladium and was subjected to leaching, reduction, and regeneration to recover metallic palladium and the alumina support. Before analysis, the samples were dried at 105 ℃ for 4 hours and ground to a particle size of less than 100 μm to ensure uniformity.

Leaching of palladium from the spent catalyst was carried out using a mixture of hydrochloric acid (6 M) and sodium hypochlorite (10%) at 80–85 ℃ for 2 hours under constant stirring. After filtration, the palladium-rich solution was reduced using zinc powder to obtain metallic palladium. For comparison, sodium formate and hydrazine hydrate were also tested as alternative reducing agents. The precipitated palladium was filtered, washed repeatedly with deionized water until neutral pH, and dried in a vacuum oven at 100 ℃ for 3 hours.

After leaching, the γ-Al_2O_3 support was separated, washed thoroughly, and calcined at 500 ℃ for 5 hours to restore its surface characteristics.

Surface morphology and microstructural features of regenerated palladium and the Al_2O_3 support were studied using a Tescan Vega 3 scanning electron microscope equipped with an Oxford Instruments EDS detector. Imaging was performed at an accelerating voltage of 15–20 kV with a working distance of 10 mm. Elemental composition was determined at three representative points, and quantitative data were obtained using INCA software. Certified standards (SiO_2, FeS_2, NaCl, Zn, Pd) were used for calibration with an accuracy of ±2 wt%.

Phase analysis of the spent catalyst, isolated palladium, and regenerated Al_2O_3 was performed on a Shimadzu XRD-7000 diffractometer using Cu Kα radiation (λ = 1.5406 Å) at 40 kV and 30 mA. Data were recorded in the 2θ range of 20 °–90 ° at a scanning rate of 2 ° per minute. Crystallinity and amorphous content were determined using HighScore Plus software with Rietveld refinement and reference patterns from the ICDD PDF-2 database.

Residual sulfur, chlorine, and zinc impurities were detected by EDS and verified by spectral analysis. Additional purification tests were carried out with concentrated nitric acid followed by repeated SEM–EDS examination. The obtained data provided a complete assessment of regeneration efficiency and impurity removal.

All measurements were performed in triplicate, and the mean values were calculated with deviations not exceeding ±3%. The SEM–EDS–XRD results were used to evaluate the morphology, metal dispersion, and phase stability of the regenerated catalyst system.

3. The Results

The results of component analysis at point 1 (Figure 1, Table 1) show that the isolated sample was not completely free of sulfur impurities after filtration. Due to poor (insufficient) washing of the precipitate of the separated metal, Cl–and Zn^{+2} ions constitute the highest content (22%) of all impurities in the processed product. To reduce or completely remove the impurities present, thorough washing of the (final) precipitate is required. However, care should be taken to avoid excessive water consumption, which is undesirable from a technological standpoint. Therefore, zinc powder should probably not be used as a reducing agent, although satisfactory results are obtained. It is advisable to use recommended reducing agents for Pd^{+2}, such as sodium formate or hydrazine hydrate, which convert to gaseous products (CO_2, N_2) after the reaction. This allows for higher palladium recovery without contaminating the palladium with reducing agent compounds [5,6,7,8].

Based on the initial chemical analysis data of the spent catalyst sample, sulfur is present up to 3%, which is confirmed by the spectral data (S=3.1%). This indicates the presence of this element as a deposit formed during catalyst operation, i.e., as the catalyst's core, which was not removed from the original catalyst sample during purification with sodium hypochlorite.

The use of NaClO and HCl solutions during the processing of the spent catalyst did not completely remove sulfur and its compounds, as evidenced by the analysis results presented in Tables 1–4 and Figures 5–8. Therefore, it is necessary to thoroughly clean the original sample from sulfur deposits before starting the processing, which is required according to the standard procedure for extracting the active catalyst component.

Table 1. The results of 1 point SEM analysis of the isolated sample Pd

Element	Signal type	Line	Apparent concentration	K–Ratio	Wt%	Wt% Sigma	Standard name	Factory standard
O	EDS	K series	3.64	0.01225	17.46	0.37	SiO2	Yes
Al	EDS	K series	0.22	0.00155	0.74	0.08	Al2O3	Yes
Si	EDS	K series	0.64	0.00509	1.86	0.08	SiO2	Yes
S	EDS	K series	1.32	0.01134	3.07	0.08	FeS2	Yes
Cl	EDS	K series	9.60	0.08392	22.32	0.22	NaCl	Yes
Zn	EDS	K series	9.06	0.09058	22.19	0.33	Zn	Yes
Pd	EDS	L series	10.51	0.10512	32.36	0.40	Pd	Yes
Total					100.00			

Table 2. The results of 2–point SEM analysis of the isolated Pd sample

Element	Signal type	Line	Apparent concentration	K–Ratio	Wt%	Wt% Sigma	Standard name	Factory standard
O	EDS	K series	2.96	0.00997	15.03	0.37	SiO2	Yes
Al	EDS	K series	0.18	0.00126	0.64	0.08	Al2O3	Yes
Si	EDS	K series	0.71	0.00565	2.18	0.08	SiO2	Yes
P	EDS	K series	0.05	0.00030	0.10	0.06	GaP	Yes
S	EDS	K series	1.17	0.01010	2.89	0.08	FeS2	Yes
Cl	EDS	K series	10.25	0.08958	25.18	0.25	NaCl	Yes
Zn	EDS	K series	9.46	0.09462	24.34	0.34	Zn	Yes
Pd	EDS	L series	8.96	0.08965	29.64	0.43	Pd	Yes
Total					100.00			

Unlike the initial catalyst composition data, the final processed product contains 1.9% silicon. The presence of silicon in the Pd^0 solid residue is apparently related to contamination by silicon compounds during the thermal processing of the intermediate product, which was precipitated after the decomposition of palladium (II) dimethylglyoximate and subjected to attempted palladium reduction in a porcelain crucible at 700 ℃ [8,9,10,11].

This indicates that the dimethylglyoximate precipitate should not be decomposed by thermal treatment at such a high temperature, as this is undesirable for two reasons: additional unwanted contamination and excessive energy consumption during palladium recovery, which leads to an impractical increase in the cost of the final product.

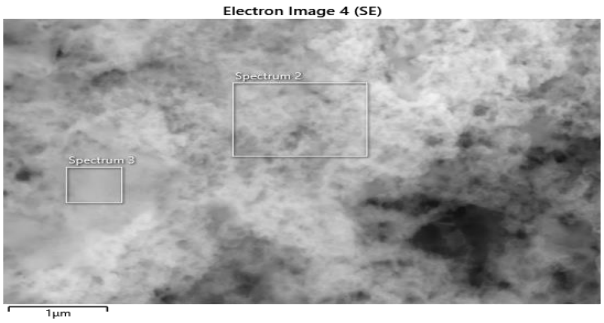

Figure 3. 2–point SEM analysis of the isolated Pd sample

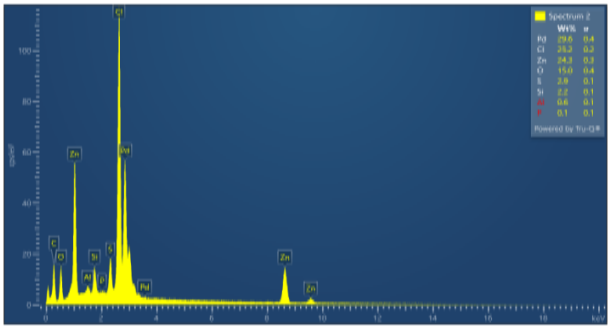

Figure 4. 2–point SEM spectrum of the isolated Pd sample

The most important outcome is that the selected method for processing the spent catalyst sample G–58I successfully separated the catalytic active component (Pd) from the support (Al_2O_3), increasing its content from the original 1.4–2.64% to 70–85% in the final product. The next task of the ongoing experimental research was to optimize the extraction yield of Pd^{2+} from the acid leaching products of the original sample to the maximum possible level.

Analysis of point 2 data shows that the content of the main component (Pd, 29.64%) is slightly underestimated, while the nature of the presence of impurity components (Zn, 24.34; Cl, 25.18%) is overestimated compared to point 1. The content of the remaining impurities: Al, S, and Si are close to previously detected results. Only the additionally detected small amount of phosphorus (0.10%) distinguishes the data from the first point.

The results of the analysis of the content of components in the third point of the spectrum of the final product show that the prevalence of the main impurities (Zn, 24.64; Cl, 21.97%) is close to the previous values in points 2 and 3 of the final product. The sulfur content is reduced to - 1%, and silicon is increased - 2.7%, which is unclear, phosphorus has almost not changed - 0.12%. It should be noted that the palladium content in the analyzed point is the lowest (Pd, 19.83%) compared to the two previous points.

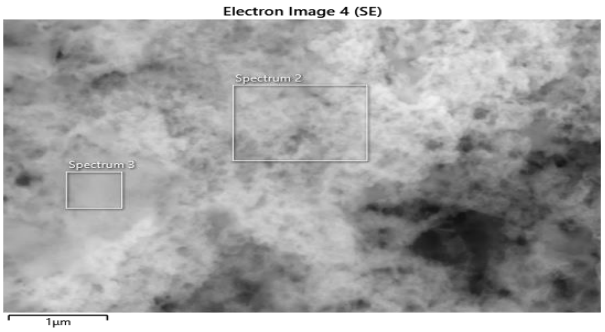

Figure 5. 3–point SEM analysis of the isolated Pd sample

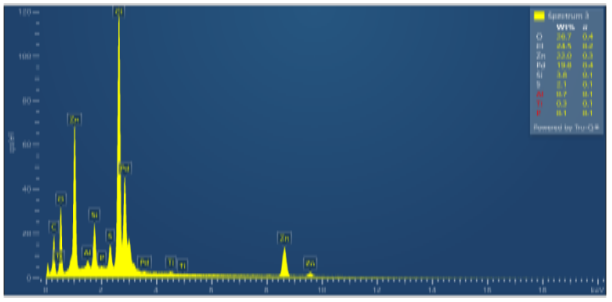

Figure 6. 3–point SEM spectrum of the isolated Pd sample

Table 3. The results of 3–point SEM analysis of the isolated Pd sample

Element	Signal type	Line	Apparent concentration	K–Ratio	Wt%	Wt% sigma	Standard name	Factory standard
Oem	EDS	K series	6.75	0.02270	26.73	0.42	SiO2	Yes
Al	EDS	K series	0.22	0.00155	0.69	0.07	Al2O3	Yes
Si	EDS	K series	1.38	0.01095	3.77	0.09	SiO2	Yes
P	EDS	K series	0.07	0.00040	0.12	0.06	GaP	Yes
S	EDS	K series	0.91	0.00785	2.07	0.07	FeS2	Yes
Cl	EDS	K series	10.84	0.09473	24.46	0.23	NaCl	Yes
Ti	EDS	K series	0.13	0.00133	0.35	0.07	Ti	Yes
Zn	EDS	K series	9.13	0.09135	21.97	0.32	Zn	Yes
Pd	EDS	L series	6.55	0.06549	19.83	0.39	Pd	Yes
Total					100.00			

Table 4

Map Sum Spectrum								
Element	Signal type	Line	Apparent concentration	K–Ratio	Wt%	Wt% sigma	Standard name	Factory standard
O	EDS	K series	35.78	0.12041	38.51	0.06	SiO2	Yes
Al	EDS	K series	0.27	0.00192	0.31	0.01	Al2O3	Yes
Si	EDS	K series	0.80	0.00635	0.78	0.01	SiO2	Yes
S	EDS	K series	1.01	0.00867	0.79	0.01	FeS2	Yes
Cl	EDS	K series	35.51	0.31032	27.78	0.04	NaCl	Yes
Zn	EDS	K series	29.79	0.29794	25.49	0.05	Zn	Yes
Pd	EDS	K series	5.88	0.05879	6.34	0.06	Pd	Yes
Total					100.00			

Unlike points 1 and 2, the last sample showed the presence of an additional minor component–titanium (Ti) at 0.35%, which is apparently related to the composition of the original catalyst sample G–58I. The aluminum content is 0.7% (equivalent to 2.64% Al_2O_3), representing the residual catalyst support. This is significantly reduced, by approximately 26.5 to 32.2 times, compared to the original amount of Al_2O_3 (70–85%) (Table 3).

According to the analysis data (Figures 5–6, Table 4), it is evident that the studied point has the lowest Pd content at 6.3%, as well as low contents of sulfur (S) at 0.8% and aluminum (Al) at 0.3%. This indicates maximum purification of the main component from sulfur deposits accumulated during the operation of the catalyst and the effective separation of the active component from the support material–Al_2O_3. The low Pd content at this point may be due to the presence of chloride ions (Cl^-) at 27.8% and zinc (Zn) at 25.5% (equivalent to ZnO at 31.78%), which together with Cl^- amount to a substantial 53.3%. Considering the oxygen content (38.5%), the total reaches 91.8%, indicating heavy contamination of the final product with these impurities.

SEM data indicate the necessity for additional chemical purification to remove the detected impurities. The most appropriate treatment may be processing the isolated sample with concentrated nitric acid followed by thorough washing of the precipitate and subsequent SEM analysis to monitor the Pd content in the resulting sample. After these additional purification steps, it is possible to obtain powder palladium with a purity of approximately 98.0%.

Therefore, it is probably not advisable to use zinc powder as a reducing agent, although satisfactory results are obtained. It is more reasonable to use recommended reducing agents for Pd^{2+} such as sodium formate or hydrazine hydrate, which converts into gaseous products (CO_2, N_2) after the reaction. This approach enables higher palladium recovery without contaminating the metal with reducer residues [1,2,3,4].

These results are confirmed by X–ray diffraction data of samples of spent catalyst G–58I (Figure 7), isolated after leaching of palladium (Figure 8) and the carrier–Al_2O_3 (Figure 9).

As seen in Figure 7, the spent catalyst sample G–58I contains impurities (S–1.2%, Fe–5.2%) and the main components Al_2O_3 (92.2%) and Pd (1.4%). After leaching, these components are absent in the support Al_2O_3 (Figure 9), which indicates the complete leaching of Pd (Figure 8) and impurity components from the spent catalyst sample G–58I.

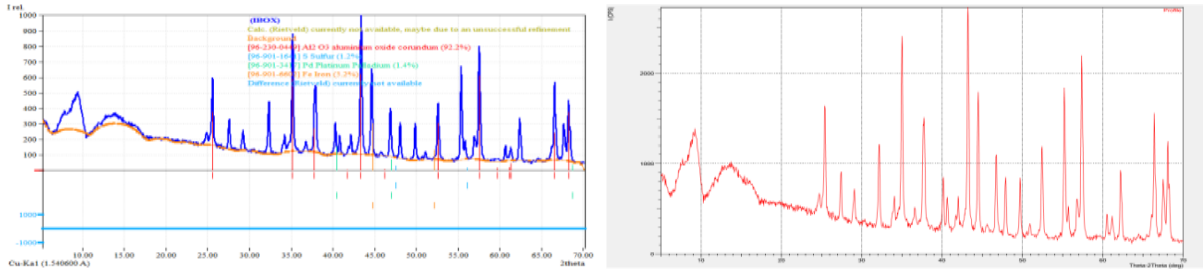

Figure 7. X–ray phase analysis (XRD analysis) of the spent catalyst G–58I

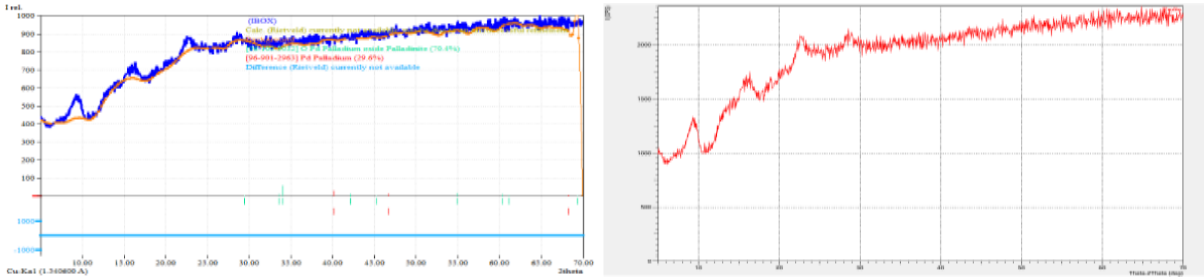

Figure 8. X–ray phase analysis (XRD analysis) of palladium isolated after leaching. Crystallinity 2.75 and amorphism 97.25%

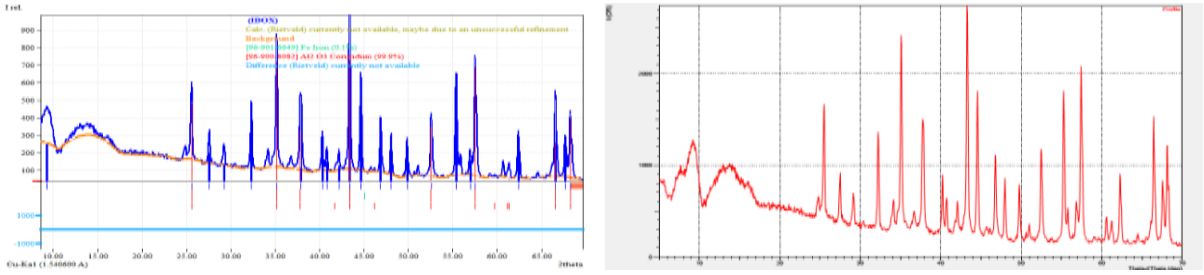

Figure 9. X–ray diffraction analysis of the purified Al_2O_3 support. Crystallinity 27.11% and amorphism 72.89%

4. Discussion

The analysis of regenerated palladium and γ-Al_2O_3 support demonstrates that the applied hydrometallurgical procedure effectively restores both the metallic phase and the carrier structure. The combined use of SEM, EDS, and XRD methods provided a comprehensive understanding of the transformation processes occurring during regeneration. Morphological examination showed that the regenerated palladium particles exhibited a more uniform surface distribution and significantly lower aggregation compared with the spent catalyst, confirming improved dispersion and reactivation of the active phase. The porous texture of the alumina support was retained, indicating that the thermal and chemical treatments did not cause destructive sintering or phase collapse [5,6,7,8,9].

The EDS data revealed that the main impurities remaining after zinc reduction were chlorine and zinc compounds, accounting for approximately one-quarter of the total mass of contaminants. This observation agrees with the known limitation of zinc as a reducing agent, which often introduces secondary contamination in the final product. When sodium formate and hydrazine hydrate were used instead, the content of residual impurities was markedly reduced, and the palladium purity increased to about 98%. This result supports the conclusion that alternative reducing agents producing volatile by-products such as CO_2 and N_2 are more efficient for obtaining high-purity palladium without solid residues.

The persistence of sulfur traces after acid leaching confirms that sodium hypochlorite and hydrochloric acid alone cannot ensure complete desulfurization. Sulfur tends to form stable deposits within the catalyst structure and may require additional oxidative pre-treatment. These findings correspond with previous studies emphasizing the necessity of preliminary sulfur removal to prevent contamination of the regenerated product and degradation of catalytic activity.

X-ray diffraction patterns confirmed the preservation of the γ-Al_2O_3 phase and the reduction of oxidized palladium species to metallic Pd^0. The presence of distinct diffraction peaks in the range of $2\theta = 40°–46°$ confirmed the metallic nature of palladium after reduction, while the γ-Al_2O_3 carrier retained its typical reflections, signifying stability under regeneration conditions. The degree of crystallinity obtained for the regenerated alumina (about 27%) and the high amorphous content (about 73%) suggest that the support maintains sufficient structural flexibility and porosity favorable for the redistribution of active metal particles.

The comprehensive data indicate that optimized regeneration not only restores the catalyst's physical integrity but also enhances its chemical and phase homogeneity. The observed increase in palladium concentration from 1.4–2.6% to 70–85% after processing demonstrates the efficiency of the chosen recovery technique. The uniform microstructure, reduction of oxidized Pd species, and preservation of the alumina framework confirm that the regenerated catalyst can be reused in multiple operational cycles without significant loss of activity.

These results have practical implications for industrial hydrometallurgical recycling, showing that the combination of controlled leaching and cleaner reducing agents can significantly lower environmental impact while increasing economic efficiency. The study thus contributes to the development of sustainable catalyst regeneration technology by emphasizing the importance of impurity control, morphological stabilization, and selection of environmentally safe reagents for palladium recovery.

5. Conclusions

The conducted physico–chemical analysis of palladium and the Al_2O_3 support after regeneration, using scanning electron microscopy (SEM), energy–dispersive X–ray spectroscopy (EDS), and X–ray diffraction (XRD), allowed a comprehensive evaluation of changes in morphology, phase composition, and elemental distribution within the catalyst structure.

SEM studies showed that regeneration promotes the restoration of the porous structure of the Al_2O_3 support, reduces the degree of palladium particle agglomeration, and provides a more uniform distribution of the active phase on the surface. The observed improvement in textural characteristics indicates the retention of a high specific surface area and accessibility of active sites for catalytic reactions. EDS results confirmed the preservation of the required palladium content in the catalyst structure and the absence of significant impurities that could adversely affect its catalytic properties. The more uniform palladium distribution on the Al_2O_3 surface after regeneration points to the effectiveness of the chosen active phase restoration method.

XRD analysis revealed that after regeneration, the main crystalline phase of the γ–Al_2O_3 support is preserved, as confirmed by characteristic peaks in the 2θ range of 20–90 °. At the same time, there is a partial decrease in the intensity of peaks corresponding to oxidized forms of palladium, which may indicate the reduction to metallic Pd^0, necessary for effective catalytic reactions.

Thus, the comprehensive physico–chemical analysis demonstrated that the regeneration process restores the essential operational characteristics of the catalyst, including the morphological stability of the support, the distribution of the active phase, and the preservation of phase composition. This creates conditions for multiple reuse of the catalyst without significant loss of its activity and selectivity, ultimately contributing to increased economic and environmental efficiency of industrial processes.

REFERENCES

[1] Kulikova M.V., Makarova A.A., Bychkov A.L. Recovery of precious metals from spent catalysts using hydrochloric acid leaching and extraction methods. Hydrometallurgy, 195, 2020, DOI: 10.1016/j.hydromet.2020.105360.

[2] Guo, J., Zhu, D., Li, C., Li, X., Liu, J. Recovery of Pd from spent Al_2O_3–supported catalysts by complexing leaching and extraction techniques. Separation and Purification Technology, 237, 2020, DOI: 10.1016/j.seppur.2019.116373.

[3] Frenzel, M., Mikolajczak, C., Reuter, M.A. Quantifying the potential for recovery of palladium from end–of–life automotive and chemical catalysts Resources. Conservation and Recycling, 143, 60–70, 2019, DOI: 10.1016/j.resconrec.2018.12.015.

[4] Cui, J., Zhang, L. Metallurgical recovery of metals from electronic waste: A Review Journal of Hazardous Materials, 158(2–3), 228–256, 2008. DOI: 10.1016/j.jhazmat.2008.02.001.

[5] Madjidova Sh. G., Rasulova Sh. N., Abdurahmanova Sh. G., Negmatov S. S. Madification of polyacrylonitrile fibre for dueing painted complex compounds on the fibre // Prog. Book of 4th Saint–Petersburg Young Scientists Conference. April 15–17, 2008.

[6] Sun Tong, Derevitskaya V. A., Rogovin Z. A. Synthesis of new derivatives of cellulose and other polysaccharides // Vysokomolsoed., 1960. – Vol. 2, No. 12. – p. 1769–1771.

[7] Lin–Yan, Derevitskaya V. A., Rogovin Z. A. Methods of synthesis of cellulose ethers with N–substituted amino acids // High–molecular compound., 1959. – No. 1., – p. 156–161.

[8] Sun Tun, Chekalin M.A., Rogovin Z.A. New method for obtaining chemically colored cellulose fibers // Highly mol. soed., 1961. – No. 10., – p. 350–355.

[9] Schrell A., Russ Werner H. Method for producing aminated cotton fibers. EPB Patent–US 5542954 A, 24.01.95.

[10] Schrell A., Huber B. Viscose fiber modified with polymeric amine compounds. Patent EPB–US 5529585 A, 07.06.95.

[11] Abdurakhmanova Sh.G., Madzhidova Sh.G., Rasulova Sh.N., Abdukadirova N. Amination of cotton fabrics with aminoalkoxysilane // Composite materials, 2010. –№1., –p. 38–43.